European Journal of Neuroscience, Vol. 25, pp. 3071–3079, 2007 doi:10.1111/j.1460-9568.2007.05573.x

Synaptic plasticity of the CA3 commissural projection in epileptic rats: an *in vivo* electrophysiological study

Claudio M. T. Queiroz and Luiz Eugênio Mello
Department of Physiology, UNIFESP-EPM, Rua Botucatu, 862-04023-062, São Paulo, SP, Brazil

Keywords: hippocampal commissural fibers, mossy fibre sprouting, paired-pulse plasticity, pilocarpine-induced status epilepticus, rat, spontaneous seizure

Abstract

The hippocampal commissural system has recently been found to participate in the generation of mirror foci after kainate-induced epileptiform discharges. In the present study we have evaluated the electrophysiological alterations in the ventral commissural hippocampal system that originates in the pyramidal CA3 cells and connects to the contralateral CA3 pyramidal cells. The recordings were performed in epileptic rats 24 h after an early behavioural spontaneous seizure between 5 and 21 days after pilocarpine-induced status epilepticus. Epileptic animals presented a marked increase in neuronal excitability after contralateral CA3 stimulation, characterized by a shift to the left in the input–output curve and the clear appearance of a population spike. Input–output curves showed that maximum population excitatory postsynaptic potential (pEPSP) amplitude was decreased by 30%, which could be related to cell death in these regions. Using paired-pulse protocols to evaluate a fast form of synaptic plasticity (i.e. paired-pulse facilitation) we observed that, despite the similar pEPSP amplitude between control and experimental groups, only epileptic animals showed strong paired-pulse population spike facilitation up to 500 ms interstimulus intervals. Despite increased excitability and pyramidal cell death, epileptic animals presented a more robust potentiation after high-frequency stimulation than controls, a protocol used to evaluate a slow form of synaptic plasticity (i.e. long-term potentiation). The increased excitability in CA3 pyramidal neurons enhanced the probability of burst activity in these neurons; this could lead to greater CA1 synchronization. The present results might have relevance for the understanding of epileptogenesis and of learning and memory deficits seen in temporal lobe epilepsy.

Introduction

A large effort has been dedicated to the understanding of neural circuits that can be reduced to slices and studied *in vitro*. While this effort has clearly provided important evidence for the role of a number of neural circuits in ictogenesis and epileptogenesis there are still potentially important circuits whose role must be teased apart. Among those are the two commissural paths connecting contralateral hippocampal structures. The first one originates from cells located in the hilar region (polymorphic layer) of the dentate gyrus and ends in the proximal third of the molecular layer of the dentate gyrus in the contralateral hippocampus (Segal & Landis, 1974). The second path originates in the pyramidal CA3 neurons and terminates in the strata oriens and radiatum in the contralateral CA3 and CA1 regions (Blackstad, 1956). While the first commissural projection inhibits contralateral dentate granular cells (Buzsaki & Czeh, 1981; Buzsaki & Eidelberg, 1981), stimulation of the CA3 region directly activates contralateral CA1 and CA3 cells via commissural projections and also indirectly activates the CA3 region via antidromic activation of contralateral CA3 fibers and/or terminals (Bliss *et al*., 1983). This connection is mainly homotopic and presents a well-defined medial–lateral distribution (West *et al*., 1979) besides the extensive intersection with the associative ipsilateral connections, the Schaffer collaterals of the same septotemporal lamella (Laurberg, 1979). Finally, the CA3 region is one of the richest portions of the hippocampus in terms of recurrent excitatory connections (Ishizuka *et al*., 1990).

A large body of evidence has indicated that the CA3 and CA1 increased excitability also contributes to seizure generation (Bernard & Wheal, 1996; Avoli *et al*., 2002; Khalilov *et al*., 2003). CA3 pyramidal cells fire bursts of action potentials (bursting mode) and provide strong and synchronous activation of CA1 pyramidal cells (Ashwood & Wheal, 1986; Wheal *et al*., 1998). Under CA3 influence, through Schaffer collaterals, CA1 neurons may become hyperexcitable and fire sustained bursts of action potentials (Traynelis & Dingledine, 1988). Sustained activation of subicular and cortical neurons by CA1 pyramidal cells may also contribute to seizure generation and neuronal synchronization. Furthermore, it has been demonstrated that CA1 pyramidal cells shift their firing mode, with a greater proportion of these cells becoming bursters in animal models of epilepsy (Sanabria *et al*., 2001; Su *et al*., 2002).

Here, we investigated the electrophysiological alterations in the pyramidal commissural path in epileptic animals. The epileptic condition was achieved by systemic administration of pilocarpine (Mello *et al*., 1993) and animals were tested ~24 h after an early spontaneous behavioural seizure. We tested the hypothesis that altered commissural CA3–CA3 connections contributed to increased excitability by the time when these early seizures emerge. We found that paired-pulse and high-frequency stimulation (HFS) of the contralateral CA3 evoked evident excitatory responses in CA3 pyramidal cells of

Correspondence: Professor Luiz Mello, as above.
E-mail: lemello@ecb.epm.br

Received 27 October 2006, revised 27 March 2007, accepted 3 April 2007

epileptic but not of control animals. Despite this altered excitability, the epileptic condition did not inhibit or attenuate HFS-induced synaptic potentiation.

Materials and methods

Male 3-month-old Wistar EPM-1 rats, weighing 250–300 g, were injected with pilocarpine (320 mg/kg, i.p., $n = 6$). Ten minutes before the pilocarpine injection, animals received methyl scopolamine (1 mg/kg, i.p.) in order to attenuate the cholinergic actions of pilocarpine in the periphery (e.g. salivation, diarrhea, etc.). In 60 min, all animals had presented orofacial myoclonus, motor seizures and status epilepticus (SE). After 90 min, animals received four doses of diazepam (5 mg/kg; interval between administrations, 2 h) to reduce the otherwise high mortality rate in this period. Animals were orally hydrated with sucrose solution and pieces of fruit were disposed in the home cage. Age-matched animals treated with vehicle (NaCl 0.9%, i.p., $n = 5$) were used as the control group. The experimental procedure was conducted under protocols approved by the Animal Care and Use Ethics Committee of the Universidade Federal de São Paulo, in accordance with the Guide for Care and Use of Laboratory Animals adopted by the National Institutes of Health. Efforts were made to reduce the number of animals used in the present experiment without compromising statistical analysis.

Five days after the SE, animals started to be video-monitored continuously (24 h/day) for the occurrence of spontaneous seizures, which appeared within ~3 weeks. After detection of the first behavioural seizure, the animals continued to be recorded until the next day, normally until the next morning (maximum 24 h between seizure detection and experimentation), to discard the acute effects of further seizure activity on the electrophysiological recordings. Animals were anaesthetized with urethane (1.5 mg/kg, i.p.) and placed in the stereotaxic apparatus. Body temperature was maintained at ~37 °C using a homoeothermic blanket control unit (Havard Apparatus, USA). One longitudinal incision in the head exposed the skull and, after the removal of musculature, two small holes were drilled, one above each of the CA3 regions (from bregma: AP, −3.6; ML, ±3.4 mm) according to a stereotaxic atlas (Paxinos & Watson, 1986). A twisted Ni-Cr wire (California Fine Wires, USA), used as a bipolar stimulating electrode ($\phi = 0.127$ mm, 500 μm tip distance), was placed in the right CA3. A stretched borosilicate capillary (World Precision Instruments, USA) filled with NaCl 0.9% with fast green (5%) was used for extracellular recordings ($R \cong 2.0$ MΩ). The recording electrode was lowered into the hippocampus using a micromanipulator (David Kopf). The two electrodes (stimulation and recording) were placed in the same coronal plane and they were finely adjusted to elicit the maximum response in both regions (Fig. 1), i.e. one positive on-going inflection with or without a fast negative component (Fig. 1C, double asterisks).

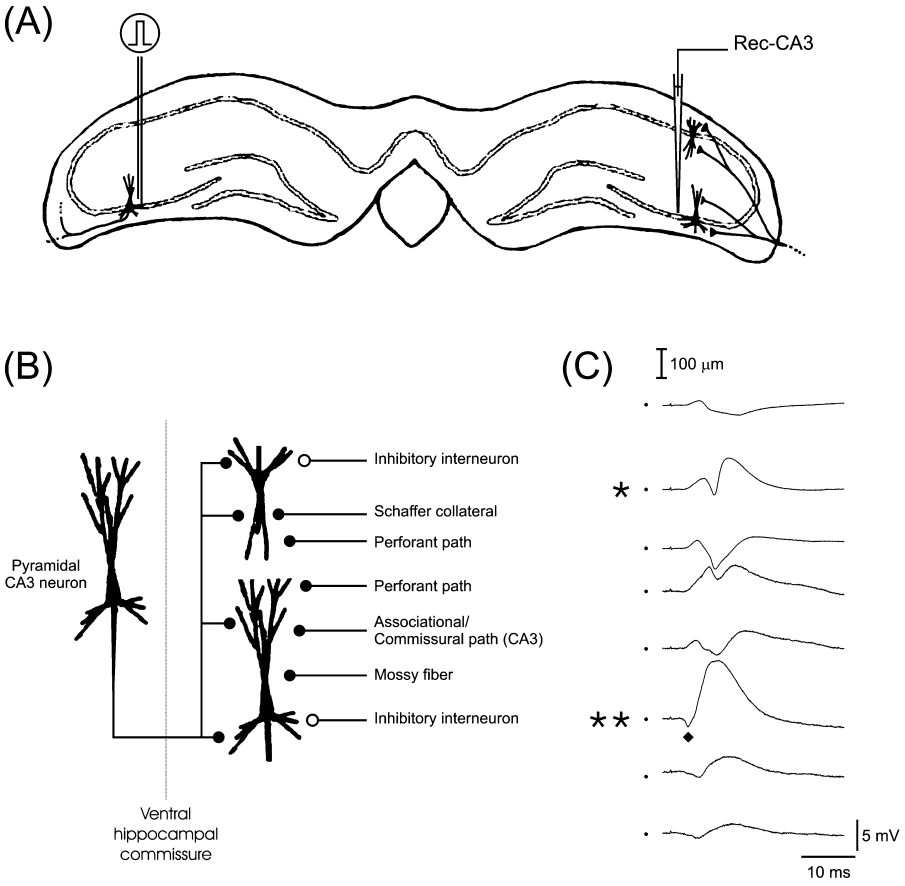

FIG. 1. Scheme presenting the anatomical background of the commissural projection. (A) Recording (right) and stimulation (left) electrode placement in the same anteroposterior axis (AP, 3.6 mm) of the dorsal hippocampus, accordingly to the stereotaxic atlas of Paxinos & Watson (1986). (B) Origin and destiny of the neuronal population stimulated in this study (mainly excitatory connections are in black, inhibitory in white). The commissural system connectivity was drawn accordingly to Blackstad (1956) and West *et al*. (1979). (C) Typical example of laminar profile of the field potential responses in the CA3 evoked by contralateral homotopic CA3 stimulation. The asterisks denote the potentials obtained at the pyramidal layers of CA1 (*, top) and CA3 (**, bottom) regions; ◆, pPVP.

Field potentials were evoked using rectangular biphasic pulse (200 μs duration) applied every 20 s (S88; Grass Instruments). The evoked responses were amplified (8700 Cell Explorer, Dagan Corporation), visualized on a digital oscilloscope (1049A; Nicolet-Thermo Electron Corporation) at 20 kHz sampling rate and recorded on floppy disks. The evoked extracellular field potentials were analysed off-line using the LTP230D program (Anderson & Collingridge, 2001; http://www.ltp-program.com). Input–output curves with fixed intensities (stimulus intensity range 200–2000 μA) were constructed to access the excitability of the commissural projection. In order to study paired-pulse facilitation and depression, double pulses at different interpulse intervals (IPIs; varying from 20 to 500 ms) at high (70%) intensity were applied. To study activity-dependent synaptic plasticity (i.e. long-term potentiation), single pulses were applied at 70% of the maximum response for 10 min (one pulse each 30 s); this was followed by applying five bursts of HFS, at 30-s intervals; each burst consisted of 50 pulses at 100 Hz. Thereafter the pre-HFS stimulation protocol was continued for at least 120 min, to detect post-HFS changes in the population excitatory postsynaptic potential (pEPSP), population prevolley potential (pPVP) and population spike (pSPK). Recordings were averaged for epochs of 5 min and are presented as ratios of the mean of pre-HFS amplitudes (for pEPSP and pPVP) or absolute increase in pSPK. We did not use the ratio for the pSPK parameter because of its low amplitude or absence before HFS. After the experiment, animals were deeply anaesthetized with thiopental (60 mg/kg, i.p.), perfused transcardially and the brains were processed for Nissl and neo-Timm staining as described elsewhere (Mello *et al*., 1993), to access cell death and mossy fibre sprouting, respectively, as well as the location of the electrodes. Supragranular mossy fibre sprouting was quantified using scores as previously described (Longo & Mello, 1997).

Field potentials were analysed according to their shape and quantified based on the amplitude and duration of the pEPSP, the amplitude of the negative pPVP and the amplitude of the pSPK in the contralateral CA3 region. The pEPSP and population prevolley magnitudes were calculated as the variation of the amplitude between the curve peak (positive and negative for the pEPSP and pPVP,

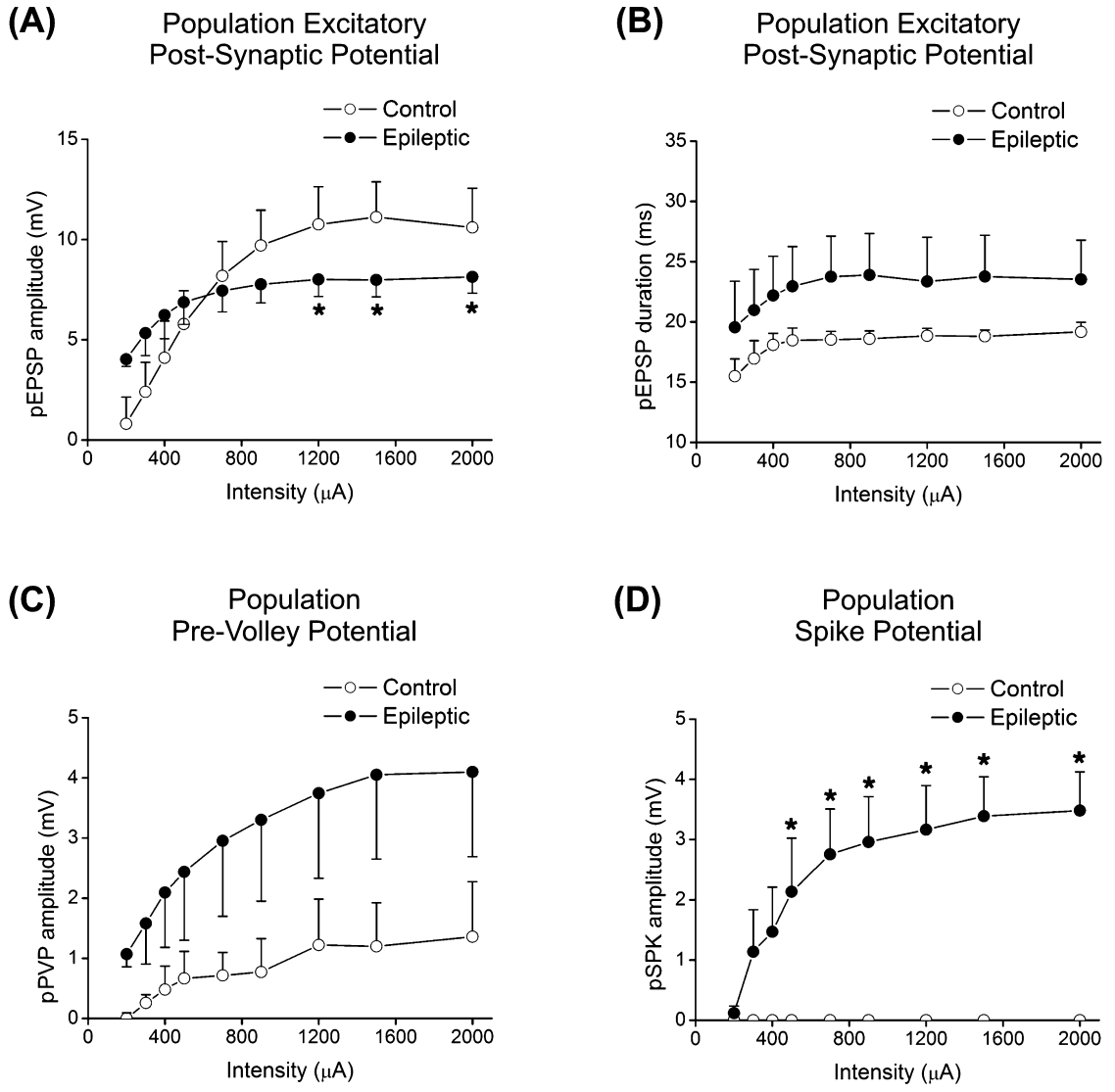

FIG. 2. Input–output curves recorded in the contralateral CA3 region. The input–output curves (200 μV to 2 mV) indicate decreased maximum (A) amplitude and (B) duration of the pEPSP, and (C) increased maximum amplitude of the pPVP in epileptic animals. (D) Increased excitability of epileptic hippocampus is based on the observation that pSPK was only presented in epileptic animals. Values represent mean ± SEM. *$P < 0.05$ compared to control group (Bonferroni–Dunn *post hoc* test).

respectively) and the average of the 5 ms that preceded the stimulation (baseline). The pSPK amplitude was measured by averaging the distance from the negative peak to the preceding and following positive peaks. The pEPSP duration was taken from a horizontal line placed at 5% of the peak pEPSP amplitude. All data are represented as mean ± SEM. Comparisons among control and epileptic animals were analysed using Student's *t*-test or ANOVA for repeated measures with the assistance of StatView software. Stimulation intensity, IPI and time were set as repeated measures. *Post hoc* comparisons were made using the Bonferroni–Dunn test. The baseline values of the long-term potentiation experiment were not included in the statistical analysis in order to evaluate the temporal evolution of the potentiation in control and epileptic animals. $P < 0.05$ was considered to be significant.

Results

Electrophysiological profile of extracellular evoked-field potential in CA3

In control animals, single test stimuli delivered to the CA3 region evoked a characteristic negative-going fast pPVP followed by a large population pEPSP in the contralateral homotopic CA3 region (Fig. 1C, double asterisks). No detectable pSPK could be recorded in control animals. In epileptic animals, the rising phase of the pEPSP was superimposed on a fast negative-going pSPK. The latencies for the peak of the pPVP were 4.73 ± 0.28 and 3.58 ± 0.17 ms ($P < 0.05$, Student's *t*-test) and for the peak of the pEPSP were 10.37 ± 0.30 and 9.34 ± 0.41 ms [not significant (NS), Student's *t*-test], for control and epileptic animals, respectively.

Input–output curves after pilocarpine-induced SE

Epileptic animals presented increased neuronal excitability in the CA3 region. This observation is based on the shift to the left of the input–output pEPSP curve (Fig. 2A), an increase in the pPVP amplitude (Fig. 2C) and the appearance of a pSPK in the CA3 region (Fig. 2D). Statistical analysis of the pEPSP, pPVP and pSPK revealed a significant group interaction with stimulation intensity ($F_{8,72} = 35.462$, 2.970 and 14.739, respectively,). This interaction reflects the fact that epileptic animals presented a 25% reduction in maximum pEPSP amplitude (the level of saturation of the input–output curve) while the amplitude of the pPVP was three times greater than in control animals (Fig. 2C). The duration of the pEPSP (Fig. 2B) was not significantly different between groups ($F_{1,9} = 1.697$; NS) nor was its interaction with stimulation intensity ($F_{8,72} = 0.377$; NS).

Paired-pulse facilitation in the commissural projection

Double-pulse stimulation was used to assess facilitation and inhibition (assumed to reflect a fast and transient form of synaptic plasticity) in the CA3 commissural projection (Fig. 3). Only facilitation was observed in response to paired pulses in both control and epileptic animals for any of the field potential parameters evaluated. Regarding the pEPSP amplitude (Fig. 4A), we found that paired-pulse facilitation was higher for IPIs of 50 and 75 ms in both control and epileptic animals. Notwithstanding, we observed a different IPI facilitation pattern between control and epileptic animals (interaction group × IPI intervals, $F_{8,72} = 6.462$, $P < 0.0001$). Epileptic animals showed 50% more facilitation for IPIs of 20 and 30 ms than did control animals ($P < 0.05$, Fig. 4A). In contrast, pEPSP duration was more facilitated in control animals (Fig. 4B; group effect, $F_{1,9} = 5.353$, $P < 0.05$). For the pPVP, we observed that as IPI decreased the facilitation became stronger (Fig. 4C; time effect, $F_{1,8} = 6.133$, $P < 0.0001$). Epileptic animals also showed a similar decrease in pPVP ratio with greater IPIs, although we only observed statistical significance for the 100 ms IPI ($P < 0.05$). The absence of pSPK in control CA3 neurons after commissural stimulation markedly differed from the evident pSPK seen in epileptic animals (Figs 3 and 4D). The largest facilitation of the pSPK amplitude occurred at 50 ms IPI, which was similar to the IPI for maximum pEPSP facilitation.

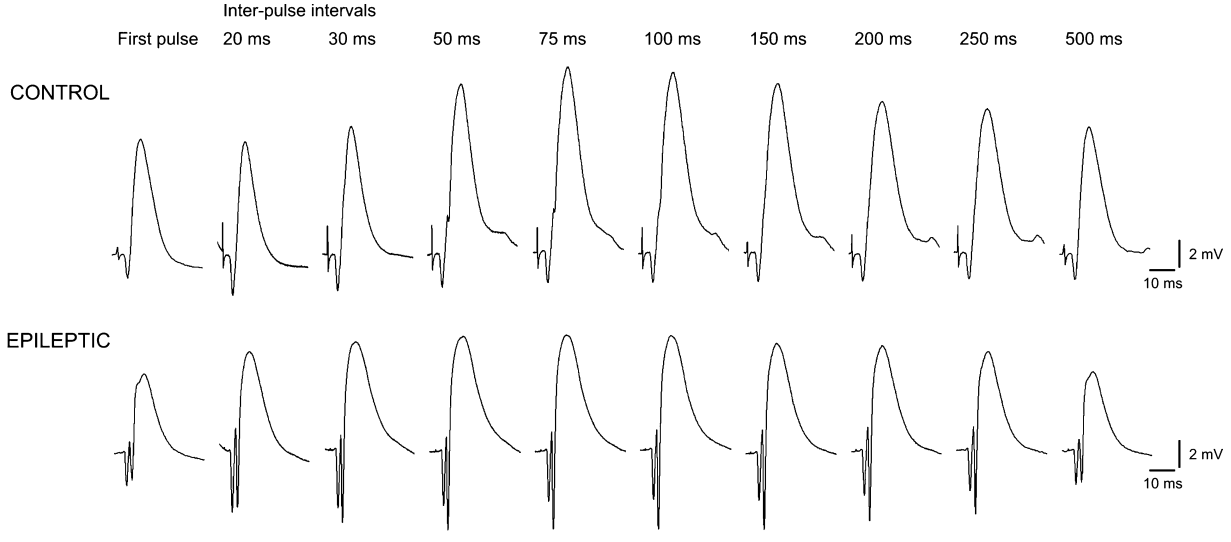

FIG. 3. Representative field potential recordings from the CA3 region after paired-pulse stimulation using different IPIs. The first trace represents the first pulse of the pair, which was similar for all the intervals analysed (the one shown here is the one from the 500-ms interval). The second pulse of the pair is in a progressive order for the interval (displayed above the curves). Both control (top) and epileptic (bottom) animals showed strong paired-pulse facilitation at all intervals studied. Quantification of the several field potential parameters is presented in Fig. 4.

Activity-dependent plasticity induced by HFS

Despite the increased excitability of the commissural projection observed in epileptic animals (Fig. 4) and decreased pEPSP amplitude (an indirect measure of neuronal depolarization; Fig. 2A), HFS stimulation of the commissural system evoked potentiation (Figs 5 and 6). pEPSP potentiation (Fig. 5A) was similar in control and epileptic animals (148.5 ± 5.2 and 166.4 ± 14.3%, respectively, mean first 30 min after potentiation; NS, Student's *t*-test). However, we did observe an interaction effect between group and time ($F_{14,126} = 1.785$; $P < 0.05$). Curiously, the pPVP (Fig. 5C) underwent depression after HFS (−43.3 ± 9.0 and −14.3 ± 4.1% for control and epileptic animals, respectively). The HFS-induced depression was much smaller in epileptic animals ($P < 0.05$ for the 10 min post-HFS). Interestingly, unlike the immediate potentiation or depression observed for pEPSP and pPVP, respectively, the amplitude of the pSPK in control animals developed slowly over the first 20 min after HFS (group × time interaction, $F_{14,126} = 3.227$, $P < 0.0001$). This effect was not observed for epileptic animals (Fig. 5D). In the first 30 min, the mean pSPK potentiation was significantly different between groups (+3.30 ± 0.91 and +5.91 ± 0.57 mV for control and epileptic animals, respectively; $P < 0.05$ for the 10 min post-HFS). For none of the parameters quantified, however, was the HFS-induced synaptic plasticity maintained at the end of the 2-h recording period (including for controls; Fig. 5). Multiple or desynchronized pSPKs were never observed at any time point for either epileptic or control animals (Fig. 6).

Cell death and mossy fibre sprouting

As described previously, pilocarpine-induced SE produces intense and widespread cell death in the central nervous system (Mello *et al.*,

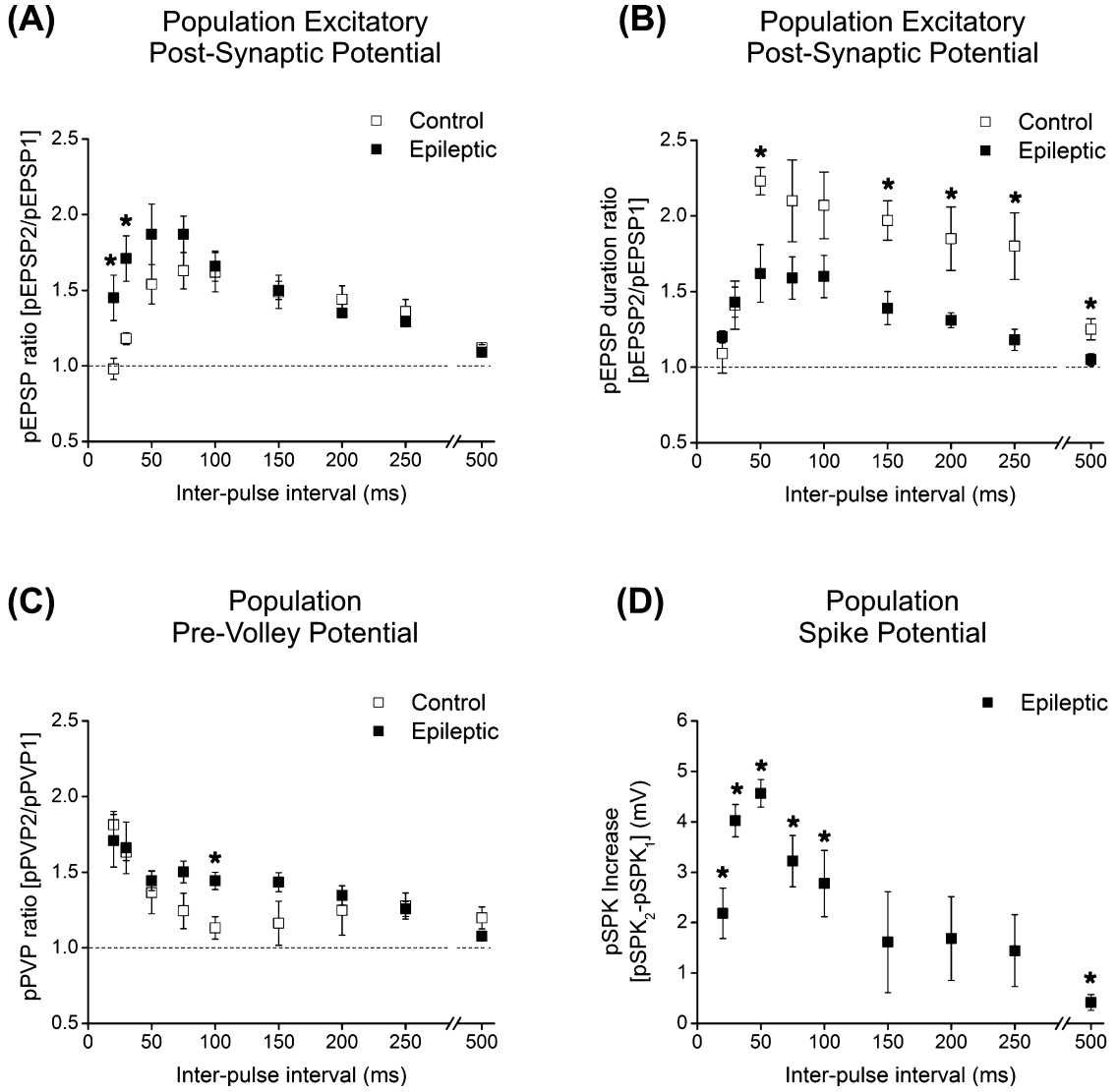

FIG. 4. Paired-pulse ratios to different IPIs in the control (□) and epileptic (■) commissural system. The contralateral CA3 neuronal population was stimulated with an intensity which evoked 70% of the maximum pEPSP response. (A) The pEPSP amplitude ratio ($pEPSP_2/pEPSP_1$) showed clear paired-pulse facilitation as the epileptic condition potentiates for short IPIs (20 and 30 ms). (B) In contrast, the pEPSP duration ratio was even more potentiated (for IPI 50 ms) in control animals than epileptic ones. (C) The pPVP ratio ($pPVP_2/pPVP_1$) showed strong paired-pulse facilitation for short IPIs (50 ms). Note that the pPVP facilitation does not match with the pEPSP facilitation seen in A, which suggests postsynaptic mechanisms involved in the pEPSP facilitation in CA3. (D) PSPK variation ($pSPK_2 - pSPK1$) presents similar pEPSP IPI profile with strong potentiation at 50 ms. Note that control animals do not present pSPK in either stimuli. Values represent mean ± SEM. *$P < 0.05$ compared to control group (Bonferroni–Dunn *post hoc* test).

1993; Covolan & Mello, 2000). Cell loss was more abundant in the hilus of the dentate gyrus but it was also observed to a lesser extent in CA3, CA1 and subicular regions. Figure 7 clearly shows the reduction in the pyramidal cell layer width of the CA3 region (Fig. 7A and B). Note that shrinkage was more abundant in the CA3b portion (Fig. 7C and D). Hippocampus from epileptic animals also presented extensive gliosis (Fig. 7, asterisks). We also observed the almost complete disappearance of hilar neurons and subtle granular cell layer dispersion in epileptic animals (data not shown). To assess the temporal development of the synaptic reorganization in the epileptic brain we evaluated aberrant mossy fibre sprouting in the inner molecular layer of the dentate gyrus (Longo *et al*., 2003). Although the animals had already presented their first spontaneous behavioural seizure, we observed only mild aberrant mossy fibre sprouting in the inner molecular layer of the dentate gyrus (data not shown), i.e. mossy fibre sprouting was far from its maximum (median mossy fibre sprouting score of 1; range from 0 to 1.5, as previously described by Longo & Mello, 1997). No alterations in the mossy fibre terminals in the hilus or in the strata oriens, pyramidale and lucidum of the CA3 were detected (data not shown).

Discussion

In the present study we showed that epileptic animals, by the time of the first behavioural spontaneous seizures, already show increased commissural excitability and facilitated pPVP in the CA3 pyramidal region. The stimulation paradigms (paired-pulse stimulation and HFS) used here showed that the CA3–CA3 commissural projection in epileptic animals presents increased paired-pulse facilitation (higher at shorter paired-pulse intervals; IPI ≤ 50 ms) and stronger potentiation just after HFS. We discuss the present results in the light of how the commissural CA3 pathway may contribute to neuronal synchronization and network excitability and, consequently, triggering of spontaneous seizures.

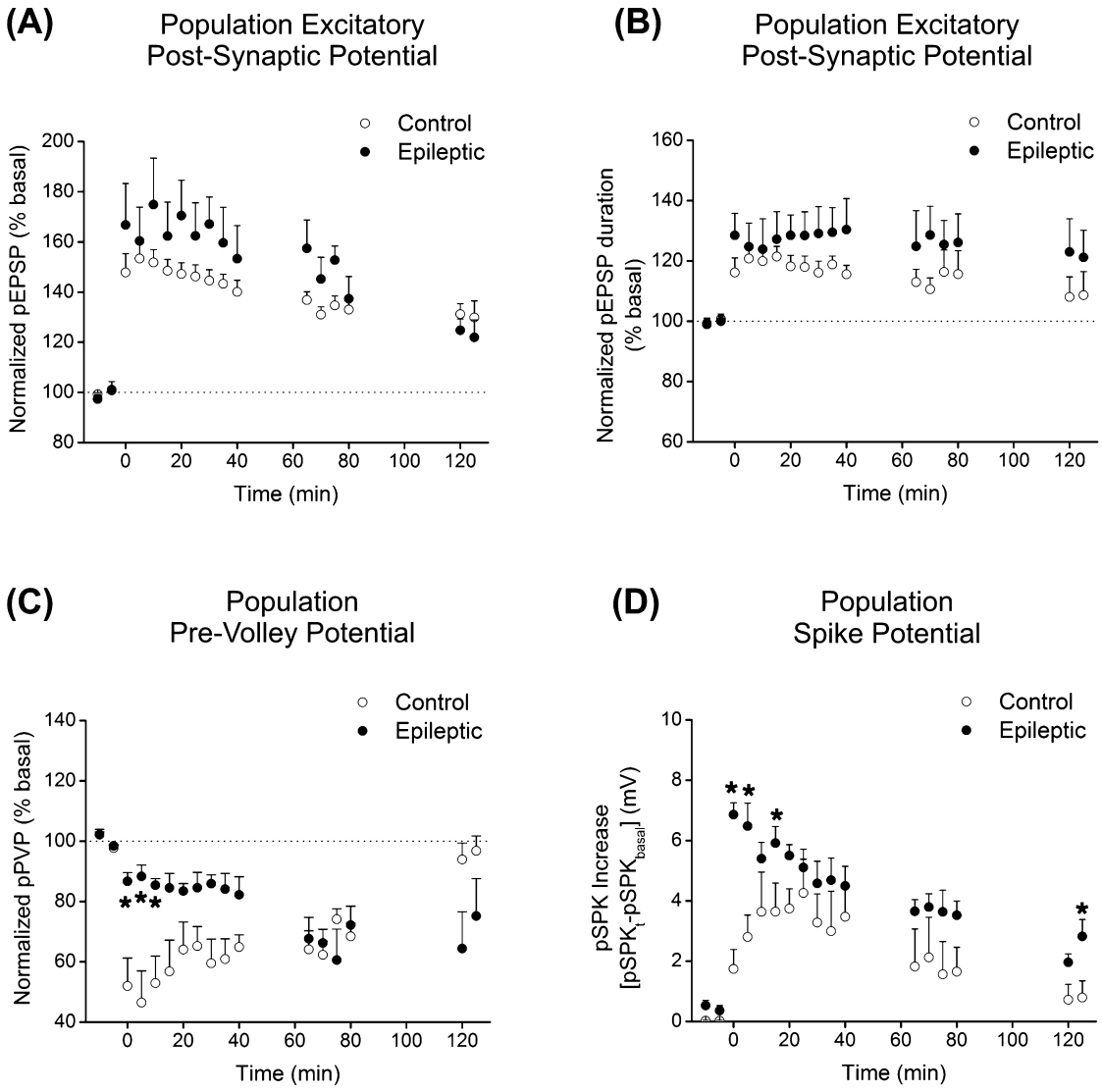

FIG. 5. Activity-dependent plasticity of the commissural system. Graphs showing the change in amplitude of (A) the pEPSP amplitude and (B) the pEPSP duration, (C) pPVP and (D) pSPK after the HFS protocol at time t = 0. Both groups of animals presented pEPSP and pSPK potentiation and pPVP depression that slowly returned to baseline values (pre-HFS) during the recording session (120 min). The pPVP depression was smaller and the pSPK potentiation was higher in epileptic animals during the first 20 min after HFS. Values represent mean ± SEM. *$P < 0.05$ compared to control group (Bonferroni–Dunn *post hoc* test).

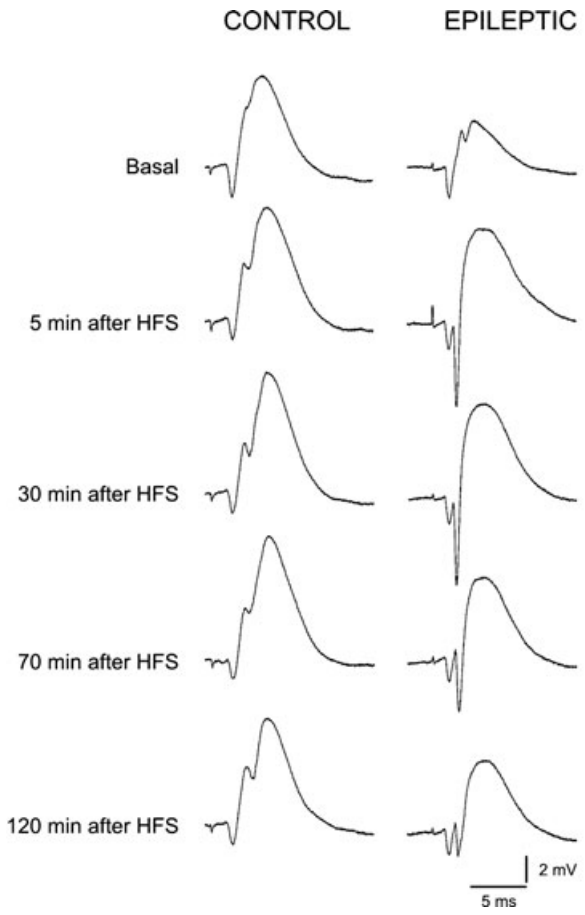

FIG. 6. Representative field potential recordings obtained in the CA3 region before (baseline) and after (5, 30, 70 and 120 min) contralateral HFS in control (left) and epileptic (right) animals.

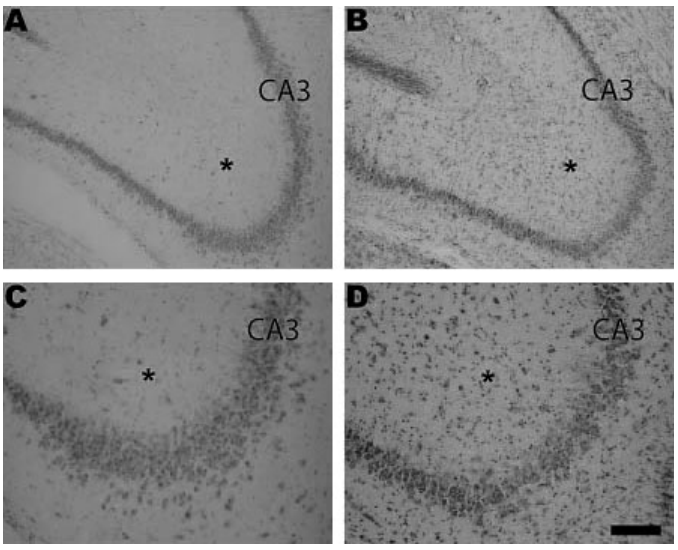

FIG. 7. Representative photomicrographs of Nissl-stained sections of the CA3 region of (A and C) control and (B and D) epileptic animals. In B note the presence of gliosis (*) in an epileptic animal as compared to the lack of such cell proliferation in controls animals as shown in A. In D, note the presence of pyramidal cell layer atrophy in the CA3b portion of an epileptic animal as compared to controls (C). CA3 depicts the pyramidal cell layer. Calibration bar, 300 μm (A and B), 150 μm (C and D).

I/O curve: increased excitability in epileptic animals

Pilocarpine-induced SE produces massive cell loss in different brain areas (Turski *et al*., 1989). In the hippocampus, although the neuronal death is preferentially of hilar neurons of the dentate gyrus (80% of such cells lost), it also occurrs in principal neurons of the pyramidal layers of CA3 and CA1 (20–30%; Covolan & Mello, 2000). Using CA3 contralateral stimulation as a paradigm to isolate the homotopic commissural connections, we observed a slight decrease in the pEPSP amplitude at maximum intensity stimulation in the CA3 region (Fig. 2A). This decrease in the pEPSP amplitude could be related to the diminished target neurons at the recording site and consequently fewer electrical generators (neurons responding to electrical activation of contralateral CA3). This conclusion is supported by the fact that reduced pEPSP amplitude after maximum stimulation intensity was also observed in the CA1 region (data not shown). This pronounced pEPSP reduction at maximum stimulus intensities was also accompanied by an increased pPVP in epileptic animals (Fig. 2C) and diminished latency for the peak of this evoked field potential within the CA3 region. The altered synaptic efficiency might suggest an altered subunit composition that in turn could account for the slight shift to the left of the input–output curve at lower intensities ($I < 500$ μA; Fig. 2A) and the observed increased excitability at the commissural projection. This assertion is fully corroborated by the outbreak of a pSPK in epileptic animals (Fig. 2D) and is suggestive of neuronal reorganization (Siddiqui & Joseph, 2005).

Hippocampal CA3 pyramidal cells present high collateral connectivity with other CA3 cells (MacVicar & Dudek, 1980; Traub & Jefferys, 1994) which, under excitatory drive, results in synchronized network activity (Bains *et al*., 1999). As no pSPK was ever observed in the CA3 region of control animals, the occurrence of pSPK in epileptic animals means that increased excitability in commissural projection leads to CA3 output and then abnormal propagation of information along other hippocampal structures, i.e. the CA1 region. In fact, enriched connectivity of recurrent glutamatergic connections between CA3 pyramidal cells facilitates network synchronization in organotypic culture (De Simoni *et al*., 2003). Consequently, our data indicate that the integrative properties of the commissural CA3–CA3 pathway are completely modified after the first spontaneous behavioural seizure in the pilocarpine-induced SE model, although we cannot rule out the possibility that this alteration was already present, in a latent state, before the first spontaneous seizure.

IPI curve: feedback and feedforward modulation

To better address the plastic properties of the commissural pathway we performed paired-pulse stimulation in order to evaluate the amount of feedforward and feedback control accompanying contralateral CA3 activation. In control animals, we found that the CA3–CA3 commissural projection is characterized by strong paired-pulse facilitation (Fig. 3). In accordance with the increased excitability observed in the I/O curve, epileptic animals presented an even greater paired-pulse facilitation, mainly at IPIs < 50 ms. The paired-pulse facilitation of the pEPSP duration (Fig. 4B) in control animals may be related to the increased pEPSP duration of the first pulse (Fig. 2B), which argues for more prolonged conductances in CA3 neurons in epileptic animals. Further evidence of potentiation is that pSPK was evoked by the second pulse (Fig. 4D) for all IPIs tested (max 500 ms). This abnormal facilitation could endure synchronization of pyramidal cells in both hemispheres, making the two hippocampi act as a single oscillator

(Fernandes de Lima *et al*., 1990; Avoli *et al*., 2002; Khalilov *et al*., 2003).

Despite the increased amplitude of the second pPVP as compared to the first, we did not observe any significant alterations in the pPVP paired-pulse ratio in pilocarpine-treated rats as compared to controls (Fig. 4C). Both control and epileptic animals showed increased paired-pulse facilitation for shorter intervals. The observation that smaller IPI intervals produce marked facilitation of the pPVP is in agreement with the idea of increased release probability due to residual Ca^{2+} ions in the presynaptic terminal from the first pulse when the second stimulus of the pair arrives (Katz & Miledi, 1968; Stuart & Redman, 1991). The fact that we observed the maximum pEPSP amplitude and pSPK paired-pulse facilitation at an IPI of 50 ms suggests that commissural projection may became highly excitable at frequencies ~20 Hz, which may contribute to hipocampal synchronization (Miles & Wong, 1987; Traub *et al*., 1995). However, could this shift towards excitation in short-term plasticity lead to impaired long-term plasticity?

HFS potentiation: synaptic plasticity was still present in epileptic animals

In order to evaluate this question, we performed HFS-induced potentiation of the commissural CA3 pathway. Associative and NMDA-dependent long-term potentiation has been previously described in the commissural CA3 projection (Chattarji *et al*., 1989; Derrick & Martinez, 1994, 1996; Martinez *et al*., 2002). As previously observed (Goussakov *et al*., 2000), the potentiation of the pEPSP did not differ between control and epileptic animals. In fact, it was the pSPK, which stands for the excitability of the neuronal ensemble, which was more potentiated in epileptic animals (Figs 5D and 6). Curiously, we observed a slowly developing potentiation of the pSPK in control commissural CA3 projections; it has been suggested that this is a non-NMDA-dependent form of synaptic plasticity (Bliss & Collingridge, 1993; Bortolotto & Collingridge, 1993; Collingridge & Bliss, 1995). One possible explanation for the present results may be the fact that high-frequency stimulation (> 10 Hz) in the CA3 region produces facilitation but also inhibition of stratum oriens synapses over pyramidal neurons (Aaron *et al*., 2003). Given the reported loss of several interneuronal cell types following pilocarpine-induced SE (Houser & Esclapez, 1996; Hamani *et al*., 1999), the absence of the slowly developing potentiation in the epileptic animals may be related to a diminished inhibitory tonus in the CA3 region of these animals just after HFS. On the other hand, as control animals still present inhibitory synapses that impinge on pyramidal neurons that can undergo potentiation (Aaron *et al*., 2003), we encountered a slowly developing potentiation after HFS. Together with our I/O and paired-pulse results (increased excitability of CA3 pyramidal neurons), this statement suggests that stratum oriens interneurons are less active in epileptic animals and may be of some relevance in pyramidal CA3 network synchronization in epileptic animals.

Conclusion

Several *in vivo* and *in vitro* electrophysiological studies have attempted to establish a casual linkage between neuronal cell loss and the subsequent formation of aberrant axonal connections. The altered physiology of the commissural pathway may lead to increased neuronal synchronization of CA3 pyramidal neurons reaching the network threshold for the seizure activation (Wozny *et al*., 2005) or interictal spikes (Traynelis & Dingledine, 1988; Traub & Dingledine, 1990; Avoli *et al*., 2002; Avoli *et al*., 2005). Much attention has been devoted to the dentate gyrus mossy fibre sprouting (Wuarin & Dudek, 1996), but enhanced connectivity has also been described in CA1 and CA3 regions (Perez *et al*., 1996). It has recently been suggested that mossy fibre–CA3 (Biagini *et al*., 2005) and Schaffer collateral–CA1 pathways (Ang *et al*., 2006) are hypoactive in epileptic animals and this reduced activity might impair the ability to control hipocampal oscillation after entrained epileptiform synchronization arriving from the entorhinal cortex (Trevino *et al*., 2007). Here, we provide evidence of increased excitability combined with enhanced feed-forward facilitation of the commissural projection in epileptic animals, which definitely affects CA3 information processing. Fast synchronization provided by the recurrent anatomy of the CA3 pyramidal neurons might contribute as an excitatory input in a sustained inhibited neuronal network in CA3. We suggest that the altered paired-pulse response of epileptic animals may predict an increased probability of hippocampal synchronization and seizure generation.

Acknowledgements

The authors would like to thank the valuable technical assistance carried out by Ms Ivone de Paulo in the preparation of the material for the histological analyses. This work was financially supported by FAPESP and CNPq. C.M.T.Q. was a FAPESP fellow (00/10826–3).

Abbreviations

HFS, high-frequency stimulation; IPI, interpulse interval; NS, not significant; pEPSP, population excitatory postsynaptic potential; pPVP, population prevolley potential; pSPK, population spike; SE, status epilepticus.

References

Aaron, G.B., Wilcox, K.S. & Dichter, M.A. (2003) Different patterns of synaptic transmission revealed between hippocampal CA3 stratum oriens and stratum lucidum interneurons and their pyramidal cell targets. *Neuroscience*, **117**, 169–181.

Anderson, W.W. & Collingridge, G.L. (2001) The LTP Program: a data acquisition program for on-line analysis of long-term potentiation and other synaptic events. *J. Neurosci. Meth.*, **108**, 71–83.

Ang, C.W., Carlson, G.C. & Coulter, D.A. (2006) Massive and specific dysregulation of direct cortical input to the hippocampus in temporal lobe epilepsy. *J. Neurosci.*, **26**, 11850–11856.

Ashwood, T.J. & Wheal, H.V. (1986) Loss of inhibition in the CA1 region of the kainic acid lesioned hippocampus is not associated with changes in postsynaptic responses to GABA. *Brain Res.*, **367**, 390–394.

Avoli, M., D'Antuono, M., Louvel, J., Kohling, R., Biagini, G., Pumain, R., D'Arcangelo, G. & Tancredi, V. (2002) Network and pharmacological mechanisms leading to epileptiform synchronization in the limbic system in vitro. *Prog. Neurobiol.*, **68**, 167–207.

Avoli, M., Louvel, J., Pumain, R. & Kohling, R. (2005) Cellular and molecular mechanisms of epilepsy in the human brain. *Prog. Neurobiol.*, **77**, 166–200.

Bains, J.S., Longacher, J.M. & Staley, K.J. (1999) Reciprocal interactions between CA3 network activity and strength of recurrent collateral synapses. *Nat. Neurosci.*, **2**, 720–726.

Bernard, C. & Wheal, H.V. (1996) A role for synaptic and network plasticity in controlling epileptiform activity in CA1 in the kainic acid-lesioned rat hippocampus in vitro. *J. Physiol. (Lond.)*, **495**, 127–142.

Biagini, G., D'Arcangelo, G., Baldelli, E., D'Antuono, M., Tancredi, V. & Avoli, M. (2005) Impaired activation of CA3 pyramidal neurons in the epileptic hippocampus. *Neuromolecular Med.*, **7**, 325–342.

Blackstad, T.W. (1956) Commissural connections of the hippocampal region in the rat, with special reference to their mode of termination. *J. Comp Neurol.*, **105**, 417–537.

Bliss, T.V. & Collingridge, G.L. (1993) A synaptic model of memory: long-term potentiation in the hippocampus. *Nature*, **361**, 31–39.
Bliss, T.V., Lancaster, B. & Wheal, H.V. (1983) Long-term potentiation in commissural and Schaffer projections to hippocampal CA1 cells: an in vivo study in the rat. *J. Physiol. (Lond.)*, **341**, 617–626.
Bortolotto, Z.A. & Collingridge, G.L. (1993) Characterisation of LTP induced by the activation of glutamate metabotropic receptors in area CA1 of the hippocampus. *Neuropharmacology*, **32**, 1–9.
Buzsaki, G. & Czeh, G. (1981) Commissural and perforant path interactions in the rat hippocampus. Field potentials and unitary activity. *Exp. Brain Res.*, **43**, 429–438.
Buzsaki, G. & Eidelberg, E. (1981) Commissural projection to the dentate gyrus of the rat: evidence for feed-forward inhibition. *Brain Res.*, **230**, 346–350.
Chattarji, S., Stanton, P.K. & Sejnowski, T.J. (1989) Commissural synapses, but not mossy fiber synapses, in hippocampal field CA3 exhibit associative long-term potentiation and depression. *Brain Res.*, **495**, 145–150.
Collingridge, G.L. & Bliss, T.V. (1995) Memories of NMDA receptors and LTP. *Trends Neurosci.*, **18**, 54–56.
Covolan, L. & Mello, L.E. (2000) Temporal profile of neuronal injury following pilocarpine or kainic acid-induced status epilepticus. *Epilepsy Res.*, **39**, 133–152.
De Simoni, A., Griesinger, C.B. & Edwards, F.A. (2003) Development of rat CA1 neurones in acute versus organotypic slices: role of experience in synaptic morphology and activity. *J. Physiol. (Lond.)*, **550**, 135–147.
Derrick, B.E. & Martinez, J.L. Jr (1994) Frequency-dependent associative long-term potentiation at the hippocampal mossy fiber-CA3 synapse. *Proc. Natl Acad. Sci. USA*, **91**, 10290–10294.
Derrick, B.E. & Martinez, J.L. Jr (1996) Associative, bidirectional modifications at the hippocampal mossy fibre-CA3 synapse. *Nature*, **381**, 429–434.
Fernandes de Lima, V.M., Pijn, J.P., Nunes Filipe, C. & Lopes da Silva, F. (1990) The role of hippocampal commissures in the interhemispheric transfer of epileptiform afterdischarges in the rat: a study using linear and non-linear regression analysis. *Electroencephalogr. Clin. Neurophysiol.*, **76**, 520–539.
Goussakov, I.V., Fink, K., Elger, C.E. & Beck, H. (2000) Metaplasticity of mossy fiber synaptic transmission involves altered release probability. *J. Neurosci.*, **20**, 3434–3441.
Hamani, C., Tenorio, F., Mendez-Otero, R. & Mello, L.E. (1999) Loss of NADPH diaphorase-positive neurons in the hippocampal formation of chronic pilocarpine-epileptic rats. *Hippocampus*, **9**, 303–313.
Houser, C.R. & Esclapez, M. (1996) Vulnerability and plasticity of the GABA system in the pilocarpine model of spontaneous recurrent seizures. *Epilepsy Res.*, **26**, 207–218.
Ishizuka, N., Weber, J. & Amaral, D.G. (1990) Organization of intrahippocampal projections originating from CA3 pyramidal cells in the rat. *J. Comp. Neurol.*, **295**, 580–623.
Katz, B. & Miledi, R. (1968) The role of calcium in neuromuscular facilitation. *J. Physiol. (Lond.)*, **195**, 481–492.
Khalilov, I., Holmes, G.L. & Ben-Ari, Y. (2003) In vitro formation of a secondary epileptogenic mirror focus by interhippocampal propagation of seizures. *Nat. Neurosci.*, **6**, 1079–1085.
Laurberg, S. (1979) Commissural and intrinsic connections of the rat hippocampus. *J. Comp. Neurol.*, **184**, 685–708.
Longo, B., Covolan, L., Chadi, G. & Mello, L.E. (2003) Sprouting of mossy fibers and the vacating of postsynaptic targets in the inner molecular layer of the dentate gyrus. *Exp. Neurol.*, **181**, 57–67.
Longo, B.M. & Mello, L.E. (1997) Blockade of pilocarpine- or kainate-induced mossy fiber sprouting by cycloheximide does not prevent subsequent epileptogenesis in rats. *Neurosci. Lett.*, **226**, 163–166.
MacVicar, B.A. & Dudek, F.E. (1980) Dye-coupling betwen CA3 pyramidal cells in slices of rat hippocampus. *Brain Res.*, **196**, 494–497.
Martinez, C.O., Do, V.H., Martinez, J.L. Jr & Derrick, B.E. (2002) Associative long-term potentiation (LTP) among extrinsic afferents of the hippocampal CA3 region in vivo. *Brain Res.*, **940**, 86–94.
Mello, L.E., Cavalheiro, E.A., Tan, A.M., Kupfer, W.R., Pretorius, J.K., Babb, T.L. & Finch, D.M. (1993) Circuit mechanisms of seizures in the pilocarpine model of chronic epilepsy: cell loss and mossy fiber sprouting. *Epilepsia*, **34**, 985–995.
Miles, R. & Wong, R.K. (1987) Inhibitory control of local excitatory circuits in the guinea-pig hippocampus. *J. Physiol. (Lond.)*, **388**, 611–629.
Paxinos, G. & Watson, C. (1986) *The Rat Brain in Stereotaxic Coordinates*. Academic Press, London.
Perez, Y., Morin, F., Beaulieu, C. & Lacaille, J.C. (1996) Axonal sprouting of CA1 pyramidal cells in hyperexcitable hippocampal slices of kainate-treated rats. *Eur. J. Neurosci.*, **8**, 736–748.
Sanabria, E.R., Su, H. & Yaari, Y. (2001) Initiation of network bursts by Ca2+-dependent intrinsic bursting in the rat pilocarpine model of temporal lobe epilepsy. *J. Physiol. (Lond.)*, **532**, 205–216.
Segal, M. & Landis, S. (1974) Afferents to the hippocampus of the rat studied with the method of retrograde transport of horseradish peroxidase. *Brain Res.*, **78**, 1–15.
Siddiqui, A.H. & Joseph, S.A. (2005) CA3 axonal sprouting in kainate-induced chronic epilepsy. *Brain Res.*, **1066**, 129–146.
Stuart, G.J. & Redman, S.J. (1991) Mechanisms of presynaptic inhibition studied using paired-pulse facilitation. *Neurosci. Lett.*, **126**, 179–183.
Su, H., Sochivko, D., Becker, A., Chen, J., Jiang, Y., Yaari, Y. & Beck, H. (2002) Upregulation of a T-type Ca^{2+} channel causes a long-lasting modification of neuronal firing mode after status epilepticus. *J. Neurosci.*, **22**, 3645–3655.
Traub, R.D., Colling, S.B. & Jefferys, J.G. (1995) Cellular mechanisms of 4-aminopyridine-induced synchronized after-discharges in the rat hippocampal slice. *J. Physiol. (Lond.)*, **489**, 127–140.
Traub, R.D. & Dingledine, R. (1990) Model of synchronized epileptiform bursts induced by high potassium in CA3 region of rat hippocampal slice. Role of spontaneous EPSPs in initiation. *J. Neurophysiol.*, **64**, 1009–1018.
Traub, R.D. & Jefferys, J.G. (1994) Simulations of epileptiform activity in the hippocampal CA3 region in vitro. *Hippocampus*, **4**, 281–285.
Traynelis, S.F. & Dingledine, R. (1988) Potassium-induced spontaneous electrographic seizures in the rat hippocampal slice. *J. Neurophysiol.*, **59**, 259–276.
Trevino, M., Vivar, C. & Gutierrez, R. (2007) Beta/gamma oscillatory activity in the CA3 hippocampal area is depressed by aberrant GABAergic transmission from the dentate gyrus after seizures. *J. Neurosci.*, **27**, 251–259.
Turski, L., Ikonomidou, C., Turski, W.A., Bortolotto, Z.A. & Cavalheiro, E.A. (1989) Review: cholinergic mechanisms and epileptogenesis. The seizures induced by pilocarpine: a novel experimental model of intractable epilepsy. *Synapse*, **3**, 154–171.
West, J.R., Nornes, H.O., Barnes, C.L. & Bronfenbrenner, M. (1979) The cells of origin of the commissural afferents to the area dentata in the mouse. *Brain Res.*, **160**, 203–215.
Wheal, H.V., Bernard, C., Chad, J.E. & Cannon, R.C. (1998) Pro-epileptic changes in synaptic function can be accompanied by pro-epileptic changes in neuronal excitability. *Trends Neurosci.*, **21**, 167–174.
Wozny, C., Gabriel, S., Jandova, K., Schulze, K., Heinemann, U. & Behr, J. (2005) Entorhinal cortex entrains epileptiform activity in CA1 in pilocarpine-treated rats. *Neurobiol. Dis*, **19**, 451–460.
Wuarin, J.P. & Dudek, F.E. (1996) Electrographic seizures and new recurrent excitatory circuits in the dentate gyrus of hippocampal slices from kainate-treated epileptic rats. *J. Neurosci.*, **16**, 4438–4448.